



## Kinetics of RDX degradation by zero-valent iron (ZVI)

Pischa Wanaratna, Christos Christodoulatos, Mohammed Sidhoum\*

Center for Environmental Systems, Stevens Institute of Technology, Hoboken, NJ 07030, USA

Available online 28 December 2005

### Abstract

Hexahydro-1,3,5-trinitro-1,3,5-triazine (RDX) is a common groundwater contaminant at military facilities. The current research has been conducted to evaluate the use of zero-valent iron (ZVI) for the remediation of water contaminated with RDX. RDX was found to degrade rapidly in the presence of ZVI. The observed first-order kinetic constant for RDX reduction follows an enzymatic-like kinetic model with respect to the ZVI concentration. At low ZVI concentrations, RDX reduction follows pseudo first order kinetics with respect to ZVI concentration; while at high ZVI concentrations the RDX reduction is zero-order. Nitroso compounds (MNX, DNX, and TNX), nitrate, nitrite and nitrous oxide were identified as the main by-products for the RDX reduction by ZVI. The nitroso compounds were found to undergo reduction by ZVI.

© 2005 Elsevier B.V. All rights reserved.

**Keywords:** RDX; Nitroso compounds; Zero-valent iron (ZVI); Kinetics; Reduction

### 1. Introduction

Past practices in ordnance production have generated explosive-laden wastewater, which was often discharged into drainage ditches, local streams, and settling lagoons. Military ordnance production facilities generate explosive-laden wastewater streams (pink water), which must be treated prior to their discharge off the plant facility limits. Pink water contains energetic materials such as TNT (2,4,6-trinitrotoluene), RDX (hexahydro-1,3,5-trinitro-1,3,5-triazine), and HMX (1,3,5,7-tetranitro-1,3,5,7-tetraazocyclooctane). Among the discharged energetic compounds, RDX is of particular environmental concern since it is known to be toxic to aquatic and terrestrial organisms. Although RDX is nonmutagenic [1], the presence of RDX in drinking water creates toxicological concerns since its ingestion adversely affects the central nervous system, gastrointestinal tract and kidneys [2]. The US EPA classifies RDX as a possible human carcinogen (Class C). In 1988, EPA also announced the lifetime Health Advisory (HA) levels for RDX to be 2 µg/L [3]. Past disposal practices have resulted in serious environmental problems and a need to develop cost effective and environmentally friendly technologies for the destruction of RDX in contaminated waters. The efficient treatment of these

waste streams contributes to the Department of Defense (DoD) sustainability and stewardship by minimizing their effect on the environment.

Activated carbon is often used for treating RDX-containing wastewaters [4]. Burrows et al. [5] determined the Freundlich isotherm constants  $K$  and  $n$  for Calgon Carbon (Filtrisorb 300) as 0.1118 and 2.938, respectively. Treatment of pink water with activated carbon is expensive and problematic, because RDX is competitively adsorbed with TNT and HMX and the exhausted carbon must be handled as hazardous waste. Nevertheless, it is still the “state-of-the-art treatment” for wastewaters from munitions production, blending, loading and packing facilities.

There were some efforts in the past to find physicochemical treatment alternatives. One alternative to activated carbon adsorption is UV radiation. Photolytic decomposition of RDX with ultraviolet-radiation (UV 254 nm) is rapid (half-life-time of 3.7 min) in water free of turbidity and other UV absorbing substances [5]. The drawback of UV-treatment is the generation of hazardous decomposition products (e.g. *N*-nitrosomethylenediamine, formaldehyde, formamide) [6,7]. Furthermore, the costs to treat large water volumes with UV-radiation might be prohibitive.

Ozone, hydrogen peroxide, iron catalyzed hydrogen peroxide (Fenton's Reaction), and chlorine have been reported as ineffective for the oxidation of RDX [8].

Freeman [9] applied surfactants to accelerate alkaline hydrolysis of RDX in wastewater and reported high reaction rates at

\* Corresponding author. Tel.: +1 201 216 5310; fax: +1 201 216 8303.  
E-mail address: msidhoum@stevens.edu (M. Sidhoum).



high pH values (10–12) and temperatures above 50 °C. Products, reaction pathways, and the kinetics of RDX alkaline hydrolysis have been studied intensively [10]. After the complete disappearance of RDX, the hydrolysis products were identified as  $\text{NO}_2^-$ ,  $\text{N}_2$ ,  $\text{NH}_3$ ,  $\text{N}_2\text{O}$ ,  $\text{HCOO}^-$ ,  $\text{CH}_2\text{O}$ , and  $\text{H}_2$ .

Substantial works strongly suggest that RDX is not degraded in aerobic, natural environment [11,12]. In contrast to the obvious recalcitrance in aerobic environments, RDX is readily degraded anaerobically in the presence of suitable organic co-substrates [12]. McCormick et al. [12] observed the production and subsequent disappearance of the mono-, di-, and trinitroso derivatives (MNX, DNX, and TNX). This indicates a reduction of nitro- to nitroso-groups as the first degradation step. The authors postulated that the ring structure becomes unstable when one nitroso group is further reduced to a hydroxylamine group, and they proposed a subsequent, spontaneous hydrolytic ring cleavage. It should be noted that non-aromatic nitroso compounds are also subject to spontaneous hydrolytic reactions themselves. This is described qualitatively and semi-quantitatively for TNX [13].  $\text{CO}_2$  and  $\text{N}_2$  were reported as the major gaseous components, while  $\text{CH}_4$  and  $\text{N}_2\text{O}$  were not detected. Hawari et al. [14] proposed that the triazine ring of RDX is cleaved through hydrolysis to form methylenedinitramine (MDNA) and bis-nitramine, which can be degraded to formaldehyde, methanol, hydrazine and dimethyl hydrazine and finally decomposed to nitrous oxide ( $\text{N}_2\text{O}$ ). Formaldehyde and methanol will eventually convert to  $\text{CH}_4$  and  $\text{CO}_2$ .

In recent years, zero-valent iron (ZVI) has been extensively studied for its ability to reduce organic pollutants [15–18]. Chemical reduction by zero-valent iron has been used in the treatment of chlorinated organics [19–22], nitroaromatic compounds [23,24], pesticides [17], explosive-contaminated soil [25], and nitrate [26]. It is commonly used as a treatment technique for contaminated groundwater. It is highly attractive since it is a passive method where no addition of electrical energy, light, or chemicals is required for the element iron to rapidly reduce the targeted compounds that come into close proximity.

The present work was carried out to determine the kinetics of RDX degradation by ZVI and to conduct a preliminary identification the reaction by-products.

## 2. Materials and methods

### 2.1. Materials

RDX was synthesized and supplied by US Army TACOM/ARDEC (Picatinny, Arsenal, NJ). The RDX had an HMX content of 10% (w/w) as production related impurity. The zero-valent iron (ZVI) in a powder form with a surface area of  $2.2 \text{ m}^2/\text{g}$  (determined by BET analysis) was obtained from ARS Technologies Inc. (New Brunswick, NJ). SEM analyses revealed that the iron particle size ranges from 3 to 12 microns. This iron powder (E-200) is manufactured by DOWA Iron Powder Co. Ltd., Japan. Reagent grade sulfuric acid was purchased from Fischer Scientific. MNX, DNX, and TNX standards were

purchased from SRI International (CA). Nitrite and nitrate standards were prepared from  $\text{NaNO}_2$  and  $\text{NaNO}_3$ . Reagent grade KOH,  $\text{NaNO}_2$ , and  $\text{NaNO}_3$  were purchased from Fisher Scientific (Springfield, NJ). Gases were obtained from Welding Supply Co. Inc. (NJ).

### 2.2. Methods of analysis

#### 2.2.1. RDX and metabolites analyses

RDX was quantified by HPLC using an Adsorbosphere C-18 10- $\mu\text{m}$  reversed-phase column (Alltech, Deerfield, IL) with pre-filter element and guard column (C-18, 5- $\mu\text{m}$ , Alltech) with an a ternary isocratic mobile phase consisting of water, methanol, and acetonitrile (40:30:30 by volume) at a flow rate of  $1.0 \text{ mL min}^{-1}$  and spectrophotometric detection at 236 nm. The retention time for RDX was 4.3 min. MNX, DNX, and TNX were analyzed using the same HPLC system with  $0.5 \text{ mL/min}$  isocratic mobile phase (65% water and 35% acetonitrile) and spectrophotometric detection at 230 nm. The retention time for MNX, DNX, and TNX were 18.95, 15.87, 13.97 min, respectively. The HPLC (Varian® Inc., Palo Alto, CA) is equipped with a ProStar 410-Auto sampler, 230-Solvent delivery system, and ProStar-330 PDA Detector with a Chromatography Workstation version 6.0 software.

#### 2.2.2. $\text{NO}_x$ analyses

Nitrite and nitrate were analyzed by ion chromatography (IC) using IonPac® AS16 (4 mm  $\times$  250 mm, DIONEX), equipped with a guard column (IonPac® AG16 (4 mm  $\times$  50 mm, DIONEX). Nitrite and nitrate were eluted by 5 mM KOH at a flow rate of  $0.8 \text{ mL/min}$  (100 mA). The retention time for  $\text{NO}_2^-$  and  $\text{NO}_3^-$  were 8.5 and 12.4 min, respectively. The IC (DIONEX IC25 Ion Chromatograph) is equipped with an AS50-Auto sampler, and LC Chromatography Endosure with a Chromelon® software.

#### 2.2.3. Gas analyses

The gaseous by-products were analyzed using FTIR (Thermo Nicolet, NEXUS 670 FT-IR) equipped with an OMNIC version 6.0a software

#### 2.2.4. TOC analyses

TOC was analyzed using a Phoenix 8000 UV-Persulfate TOC analyzer (Teledyne Tekmar Company, Mason, Ohio), equipped with a TOC boat sampler (Rosemount Dohrmann Model 183; Teledyne Tekmar Company); and a TOC talk software (Teledyne Tekmar Company, Mason, Ohio).

### 2.3. Experimental procedure

The effect of initial RDX and zero-valent iron concentrations on the kinetics of RDX destruction was studied by conducting batch experiments at room temperature. The experiments were carried out in 50-mL and 100-mL plastic bottles (Nalgene, LDPE Wide-Mouth Bottles, Fisher Scientific, Pittsburgh, PA) or 250-mL beaker. First, saturated RDX aqueous solutions were prepared by dissolving RDX powder in de-ionized (DI)

water. Since we are studying the reduction of RDX below solubility limit (38.4 mg/L at 20 °C [27]), the saturated solutions were diluted with DI water. Next, the pH of the aqueous solution was adjusted around 3 with sulfuric acid (1N). The reaction was initiated by adding zero-valent iron (ZVI). Experiments were conducted in the dark to prevent photolytic degradation of RDX. Samples (3 mL) were withdrawn periodically using a microsyringe and filtered through a 0.2 μm filter (Whatman® Puradisc, Whatman International Ltd) to remove suspended iron particles. To overcome potential RDX adsorption losses during filtration, it was necessary to discard the first mL of the filtered samples prior to HPLC analyses. All samples were analyzed in duplicate for RDX.

A three-blade propeller rotated by an overhead lab stirrer (Stirpak model 4554-10, Cole Parmer) was used to stir the mixture. The stirrer was centered and lowered into the beaker and raised to a height of 1 cm above the beaker bottom. Experiments were conducted at rotational speeds in the range of 110–700 rpm to determine the minimum speed required to overcome external mass transfer limitations.

Tumbling mixing was achieved by conducting experiments using 50 or 100 mL Nalgene bottles attached to a Rugged-Rotator (Glas-Col®, Glas-Col, LLC) and tumbled end over end at its maximum speed (83 rpm with 45° incline) to ensure proper mixing of the ZVI–water matrix.

RDX kinetic experiments were carried out at room temperature in batch mode with initial RDX concentrations ranging from 5 to 30 mg/L; and ZVI concentrations ranging from 0.002 to 7.6 M (0.0125–42.55% w/v).

### 3. Results and discussion

Preliminary experiments indicated that RDX is labile in the presence of ZVI and disappears rapidly from solution. After complete disappearance of RDX in the aqueous phase, ZVI was recovered and subjected to extraction with methanol. HPLC analyses of the methanol extract indicated that there was no RDX. Degradation experiments carried out with dissolved ZVI did not result in RDX disappearance from the bulk solution. These findings indicate that (i) the observed RDX disappearance from the bulk aqueous phase could not be attributed to physical adsorption onto ZVI, and (ii) the RDX degradation can be attributed to chemical reaction(s) mediated by the iron surface. For surface mediated reactions, reaction rates vary with catalytic surface sites and bulk-phase solute concentrations. Catalytic surface sites are proportional to the catalyst surface area and, hence the catalyst concentration. Under the assumption that the overall transformation rate is governed by the rate of surface reaction, various models have been developed to predict the kinetics of transformation of chlorinated compounds in the presence of zero-valent iron [28]. Often, pseudo-first order kinetics have been assumed to be sufficient to describe the reactions, although other models also take into account the adsorption of organic compounds to reactive and non-reactive sites on the iron surface.

Here, we assume that the reduction of RDX follows a second-order rate law with respect to the RDX and iron concentrations,

that is:

$$\frac{dC_{\text{RDX}}}{dt} = -k_2 C_{\text{RDX}} C_{\text{Fe}^0} \quad (1)$$

where  $C_{\text{RDX}}$  is the RDX concentration,  $C_{\text{Fe}^0}$  is the iron concentration, and  $k_2$  is the second-order rate constant. The second-order rate constant,  $k_2$ , cannot be determined directly as the consumption of iron with time can not be conveniently measured during the time course of the reaction. However, by adjusting the experimental conditions a pseudo-first order rate constant  $k_1$  can be obtained. This situation can be realized, by maintaining the iron concentration sufficiently in excess such that any change in the concentration of the iron is insignificant compared to the change in concentration of RDX. Therefore, under such experimental conditions where iron is well in excess, Eq. (1) is reduced to the following pseudo-first order rate equation:

$$\frac{dC_{\text{RDX}}}{dt} = -k_1 C_{\text{RDX}} \quad (2)$$

The pseudo-first order rate constant  $k_1$  is therefore composed of the second-order rate constant  $k_2$  multiplied by the concentration of elemental iron in the reacting mixture, as reflected in Eq. (3):

$$k_1 = k_2 C_{\text{Fe}^0} \quad (3)$$

By measuring the RDX concentration during the time course of the reaction, one can obtain the pseudo-first order rate constant ( $k_1$ ) using the integrated form of Eq. (2):

$$\ln C_{\text{RDX}} = \ln C_{\text{RDX}}^0 - k_1 t \quad (4)$$

where  $C_{\text{RDX}}^0$  is the initial concentration of RDX. Accordingly, the pseudo first-order rate constant,  $k_1$ , is obtained using regression analysis as the slope of the semi-logarithmic plots of concentration–time profiles for each elemental iron concentration. The kinetics of RDX reduction by ZVI, have been investigated experimentally by studying the effect of ZVI and initial RDX concentrations on the time course of RDX disappearance.

#### 3.1. Effect of mixing intensity on RDX degradation by ZVI

The mass transfer resistance external to the iron particles was assessed by comparing the extent of RDX conversion histories in batch experiments under different mixing intensities. Mixing was achieved using either a mechanical stirrer or by tumbling. The mechanical stirrer was operated at speeds ranging from 110 to 700 rpm. The extent of RDX conversion ( $\xi$ ) is defined as:

$$\xi = \frac{C_0 - C}{C_0} \quad (5)$$

where  $C_0$  is the initial RDX concentration, and  $C$  the RDX concentration at time  $t$ .

Experiments were conducted with initial RDX concentrations of 10 and 30 mg/L, and ZVI:RDX molar ratio of 3000 and 10,000, respectively. The extent of conversion with time shown in Figs. 1 and 2, suggest that external mass transfer resistance is negligible (i) at 400 rpm and above for the mechanically stirred conditions and (ii) when using the Rugged-Rotator tumbler at

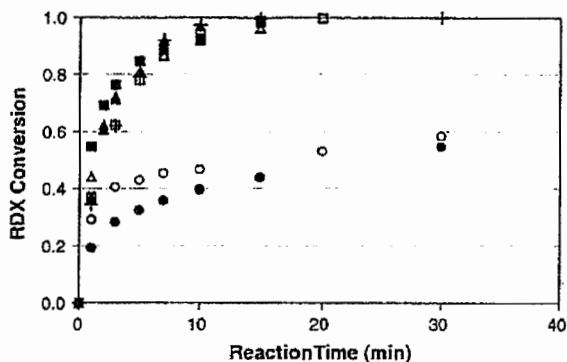


Fig. 1. Effect of mixing speed and mixing type on RDX degradation using ZVI with initial RDX concentration of 10 mg/L and a molar ratio of ZVI:RDX = 3000. (●) 110 rpm, (○) 185 rpm, (▲) 250 rpm, (+) 400 rpm, (□) 600 rpm, (△) 700 rpm, (■) Rugged-Rotator.

its maximum rotational speed. Consequently, all reaction experiments were conducted using the Rugged-Rotator operated at its maximum rotational speed.

### 3.2. Effect of ZVI loading on RDX reduction

Experiments were conducted to determine the effect of ZVI loading on the kinetics of RDX reduction. In these experiments, the initial RDX concentration was 10 mg/L and the amount of ZVI was varied from 0.05 to 1.5 g, which corresponds to ZVI:RDX molar ratios ranging from 414 to 11,400. The experimental conditions are summarized in Table 1. The data presented in Fig. 3 indicate that the RDX reduction proceeds very fast. The pseudo-first order rate constants ( $k_1$ ) obtained by linear regression (Eq. (4)) and presented in Table 1 indicate that RDX reduction by ZVI under these experimental conditions follows first-order kinetics. A plot of the pseudo-first order rate constants ( $k_1$ ) versus the corresponding ZVI molar concentration should yield, according to Eq. (4) a straight line whose slope is the second-order kinetic constant ( $k_2$ ). Fig. 4 indicates that the pseudo-first order rate constant ( $k_1$ ) varies linearly with respect to ZVI concentration ( $R^2 = 0.993$ ). Accordingly, the second-order kinetic constant ( $k_2$ ) is  $1.748 \text{ M}^{-1} \text{ min}^{-1}$ .

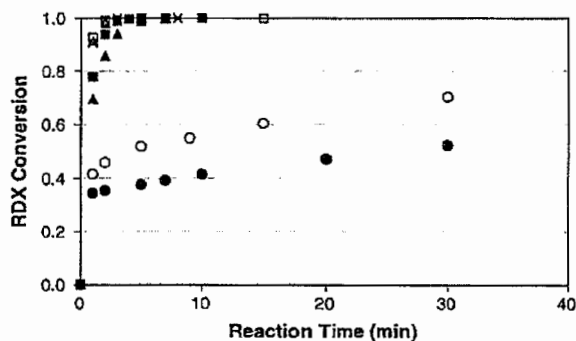


Fig. 2. Effect of mixing speed and mixing type on RDX degradation using ZVI with initial RDX concentration of 30 mg/L and a molar ratio of ZVI:RDX = 10,000. (●) 110 rpm, (○) 185 rpm, (▲) 250 rpm, (×) 400 rpm, (□) 600 rpm, (△) 700 rpm, (■) Rugged-Rotator.

Table 1  
Table of kinetic of RDX degradation using ZVI and the regression coefficient with initial RDX at 10 mg/L

ZVI loading		Initial RDX concentration		Molar ratio ZVI:RDX	$k_1$ ( $\text{min}^{-1}$ )	$R^2$
(g)	(M)	(mg/L)	(mM)			
0.05	0.02	10.25	0.05	414	0.095	0.986
0.21	0.08	11.32	0.05	1570	0.153	0.991
0.50	0.191	9.64	0.043	4402	0.406	0.986
0.75	0.29	10.38	0.05	6101	0.492	0.996
1.50	0.57	11.13	0.05	11401	0.976	0.995

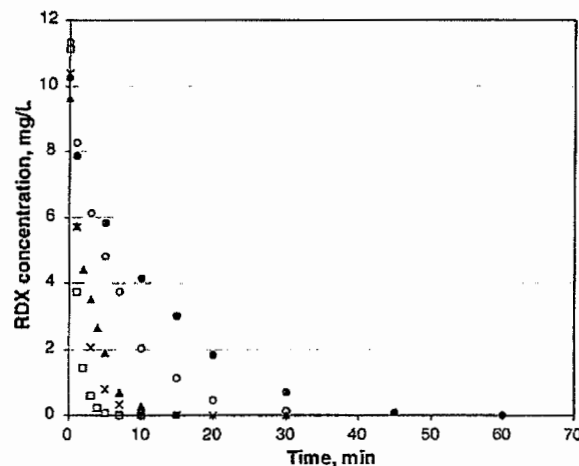


Fig. 3. Time concentration profile for RDX degradation at various ZVI concentrations with initial RDX concentration at 10 mg/L. (●) Initial RDX = 10.25 mg/L, ZVI = 0.019 M; (○) Initial RDX = 11.32 mg/L, ZVI = 0.080 M; (▲) Initial RDX = 9.64 mg/L, ZVI = 0.191 M; (×) Initial RDX = 10.38 mg/L, ZVI = 0.286 M; (□) Initial RDX = 11.13 mg/L, ZVI = 0.572 M.

### 3.3. Effect of fixed ZVI:RDX molar ratio on RDX reduction

RDX reduction experiments were conducted at a fixed ZVI:RDX ratio of 1300:1. In these experiments, the initial

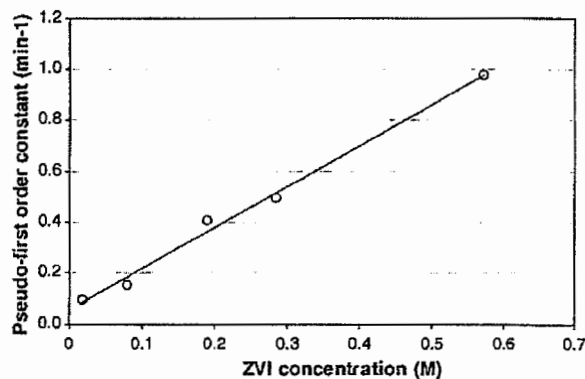


Fig. 4. Linear regression analysis using Eq. (3) for an initial RDX concentration of 10 mg/L. The second-order rate constant ( $k_2$ ) is calculated from the slopes of the curve. (○) Experimental data, (—) Linear fit ( $R^2 = 0.993$ ).

Table 2  
Pseudo-first order rate constant at a constant ZVI/RDX ratio of 1300:1 with variable initial concentrations of RDX and ZVI

ZVI (%w/v)	ZVI (M)	RDX (mg/L)	RDX (M)	Molar ratio ZVI:RDX	$k_1$	$R^2$
0.1709	0.031548	5.224	$2.35 \times 10^{-5}$	1342	0.1776	0.9927
0.3160	0.0602	9.59	$4.32 \times 10^{-5}$	1394	0.1690	0.9969
0.70	0.12924	21.72	$9.78 \times 10^{-5}$	1322	0.1802	0.9904
1.03	0.19015	32.34	$14.55 \times 10^{-5}$	1307	0.1948	0.9939

RDX concentration was varied from 5 to 30 mg/L. The time–concentration profiles for RDX disappearance in the aqueous phase and the pseudo-first order kinetic model (fitted curve) are shown in Fig. 5. Experimental conditions and the obtained pseudo-first order rate constants are presented in Table 2. The data indicate that the obtained pseudo-first order rate constants are identical for this ZVI:RDX molar ratio.

#### 3.4. Effect of initial RDX concentration at fixed ZVI loading on RDX reduction

RDX reduction experiments were carried out by varying the initial RDX concentration from 5 to 31 mg/L at a fixed ZVI loading (31.3 mM). Experimental data and the curve for pseudo-first order kinetic model are shown in Fig. 6 and Table 3 indicate that the pseudo-first order rate constants vary from 0.0177 to 0.1776  $\text{min}^{-1}$ . The highest  $k_1$  value corresponds to the lowest initial RDX concentration (5.2 mg/L) and the lowest  $k_1$  value corresponds to the highest initial RDX concentration (31.4 mg/L). These results indicate that the reaction rate is a strong function of the number of iron surface active sites, and therefore the ZVI:RDX molar ratio is an important reaction variable.

#### 3.5. Effect of high ZVI loading and fixed initial RDX concentration on RDX reduction

Since the reduction of RDX by ZVI involves surface reaction(s), the metal surface area strongly affects the RDX reduction

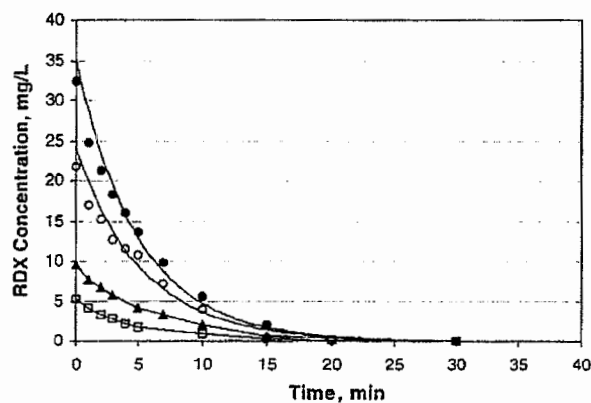


Fig. 5. Time concentration profile for RDX reduction at various initial RDX concentrations at a constant ZVI/RDX ratio of 1300:1. (●) Initial RDX = 5.22 mg/L, ZVI = 31.55 mM; (○) Initial RDX = 9.59 mg/L, ZVI = 60.2 mM; (▲) Initial RDX = 21.72 mg/L, ZVI = 129.2 mM; (□) Initial RDX = 32.34 mg/L, ZVI = 190.2 mM; (—) Pseudo-first order kinetic model.

kinetics. The number of available active iron sites significantly affects RDX reduction rates, and therefore increasing the concentration of ZVI in the solution will accelerate the reaction by providing more active sites. In order to study the effect of a wide range of ZVI loadings, experiments were conducted using a high RDX initial concentration (30 mg/L).

The pseudo-first order reaction rate constants,  $k_1$ , for RDX reduction at various ZVI concentrations were determined by linear regression of  $\ln(C/C_0)$  versus time from time concentration profiles. All plots were highly linear with correlation coefficients greater than 0.972. Non-linear regression of  $k_1$  versus ZVI concentration is presented in Fig. 7. Accordingly, the data shows that the pseudo-first order reaction rate constant,  $k_1$ , can be expressed using the following enzymatic-like kinetic model ( $R^2 = 0.988$ ):

$$k_1 = \frac{k_{\max} [\text{ZVI}]}{k_0 + [\text{ZVI}]} \quad (6)$$

where  $[\text{ZVI}]$  is the ZVI dosage (M),  $k_1$  ( $\text{min}^{-1}$ ) is the pseudo-first order rate constant, the regression constants  $k_{\max}$ , and  $k_0$  are 2.824 ( $\text{min}^{-1}$ ) and 1.806 (M), respectively. This indicates that although the reduction reaction is pseudo-first order with respect to RDX concentrations; it follows pseudo-first order kinetics with respect to ZVI concentrations at low ZVI loadings; and zero order kinetics with respect to ZVI concentrations at very high ZVI loadings.

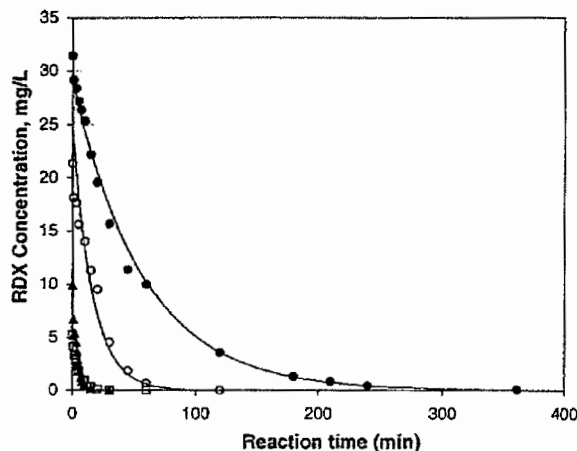


Fig. 6. Time concentration profile for RDX reduction at various initial concentrations and fixed initial amount of ZVI. Initial ZVI concentration 0.175% w/v (31.33 mM). Initial RDX (mg/L): (●) 5.2, (○) 9.2, (▲) 21.3, (□) 31.4; (—) Pseudo-first order kinetic model.

Table 3

Pseudo-first order rate constant at ZVI/RDX ratio ranging from 223:1 to 1342:1 with fixed initial amount of ZVI (31.33 mM)

ZVI (g)	V sol (mL)	ZVI (mM)	RDX (mg/L)	RDX (M)	Molar ratio ZVI:RDX	$k_1$	$R^2$
0.1709	97	31.55	5.22	2.35E-05	1342	0.1776	0.9927
0.0842	47	32.08	9.18	4.13E-05	777	0.1567	0.9873
0.17109	97	31.58	21.34	9.603E-05	329	0.0606	0.9959
0.1709	97	31.55	31.41	14.13E-05	223	0.0177	0.9975

### 3.6. Characterization of the by-products resulting from the reduction of RDX by ZVI

Analyses of the reactor head-space by FT-IR (Nicolet FT-IR Spectrometers, Thermo Electron Corp.), indicated that nitrous oxide ( $N_2O$ ) was produced; however neither  $CO_2$  or  $NH_3$  were detected. In all RDX reduction experiments, it was found that the total organic carbon (TOC) remained constant, which confirms the FT-IR analyses that the carbon was not converted to  $CO_2$ . This suggests that RDX breaks down to smaller organic molecules in the dissolved phase which ZVI can no longer decompose.

Nitrite ( $NO_2^-$ ) and nitrate ( $NO_3^-$ ) have been identified as by-products resulting from the reduction of RDX by ZVI. A typical nitrite and nitrate concentration profiles during the time course of the RDX reduction with ZVI (1% w/v) is shown in Fig. 8. From Fig. 8, it is observed that (i) the concentration of nitrite increases with reaction time and then reaches a plateau; and (ii) nitrite is produced in much larger quantities as compared to nitrate.

Substantial amounts of nitroso derivatives were observed. The concentration of MNX (hexahydro-1-nitroso-3,5-dinitro-1,3,5-triazine) was found to be higher than DNX (hexahydro-1,3-dinitroso-5-nitro-1,3,5-triazine), and TNX (hexahydro-1,3,5-trinitroso-1,3,5-triazine). However, after an initial increase of MNX, DNX, and TNX concentrations in the aqueous phase, it was observed that these concentrations decreased drastically during the time course of the reaction as shown in Fig. 9. This

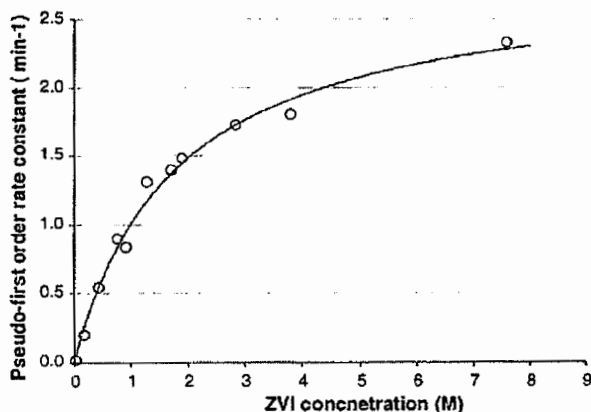


Fig. 7. Effect of ZVI concentration on the observed pseudo-first order rate constant in reactions with initial RDX concentration of 30 mg/L. (○) Experimental data, (—) Model (Eq. (6)).

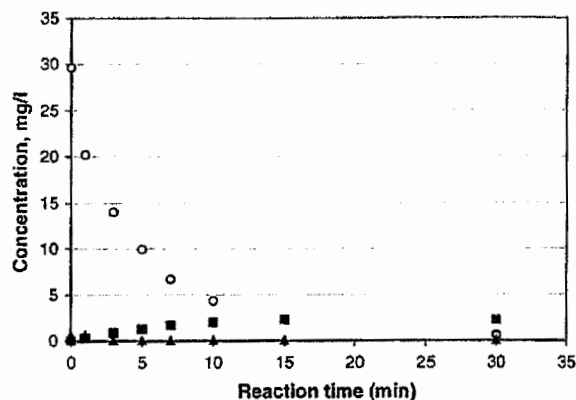


Fig. 8. RDX, nitrite and nitrate time concentration profile for initial RDX concentration 30 mg/L and 1.0% (w/v) ZVI loading. (○) RDX, (■) Nitrite, (▲) Nitrate.

might indicate that the reduction of nitro- to nitroso-groups is the first degradation step in the reduction of RDX by ZVI. The concentration of MNX was found to be higher than DNX and TNX, respectively. No attempt was made to establish a material balance since there are still some by-products that have not yet been identified.

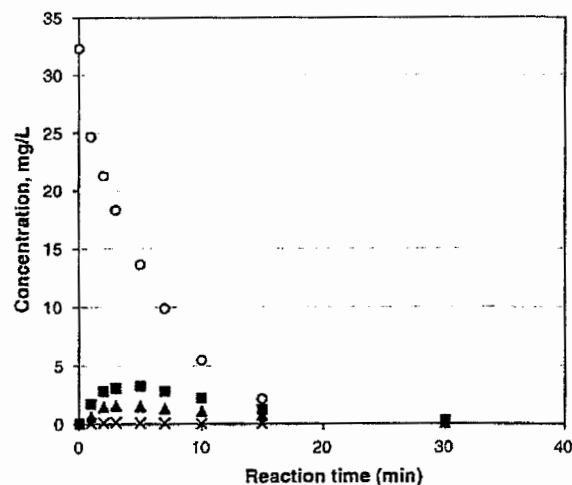


Fig. 9. RDX and RDX metabolites time concentration profiles for initial RDX concentration of 30 mg/L and 1.0% (w/v) ZVI loading. (○) RDX, (■) MNX, (▲) DNX, (×) TNX.

#### 4. Conclusions

The study shows that zero-valent iron is highly effective in degrading RDX in aqueous solution. RDX degradation rates increase with ZVI concentration. The RDX degradation is attributed to chemical reaction(s) mediated by the ZVI surface. RDX reduction by ZVI was found to follow pseudo-first order kinetics with respect to RDX concentrations. Depending on the ZVI loading, the RDX reduction follows first order kinetics with respect to ZVI at low iron loadings; and zero-order kinetics with respect to ZVI at very high iron loadings. MNX, DNX, TNX,  $\text{NO}_2^-$ ,  $\text{NO}_3^-$ , and  $\text{N}_2\text{O}$  were identified as by-products during RDX reduction by ZVI. Experimental data indicate that the RDX metabolites (MNX, DNX, and TNX) are also reduced by ZVI. Further studies are needed to identify all by-products in order to perform a material balance, and propose a mechanism for the RDX reduction by ZVI.

#### Acknowledgements

This research was supported by the DOD US ARMY TACOM/ARDEC Contract No. DAAE30-00-D-1011 #7.

#### References

- [1] E.L. Tan, C.H. Ho, W.H. Griest, R.L.J. Tyndall, *Toxicol. Environ. Health* 36 (1992) 165–175.
- [2] E.L. Etnier, *Regul. Toxicol. Pharmacol.* 9 (1989) 147–157.
- [3] U.S. Environmental Protection Agency 1988. Health Advisory for Hexahydro-1,3,5-trinitro-1,3,5-triazine (RDX). Criteria and Standards Division, Office of Drinking Water, Washington, DC.
- [4] J.W. Patterson, N.I. Shapira, J. Brown, Pollution abatement in the military explosives industry, in: *Proceeding of the 31th Industrial Waste Conference*, 1976, pp. 837–842.
- [5] W.D. Burrows, R.H. Chyrek, C.I. Noss, M.J. Small, Treatment for removal of munition chemicals for army industrial wastewaters, in: *MIDAtlantic Industrial Waste Conference, Toxic and Hazardous Wastes*, 1984.
- [6] D.J. Glover, J.C. Hoffsommer, Photolysis of RDX: Identification and Reactions of Products, Naval Surface Weapons Center, Silver Spring, MD, Technical Report NSWC TR-79-349, 1979.
- [7] D.H. Rosenblatt, E.P. Burrows, W.R. Mitchell, D.L. Parmer, *Organic Explosives and Related Compounds. The Handbook of Environmental Chemistry*, Vol. 3, Part G, Springer-Verlag, Berlin, 1991.
- [8] M.J. Semmens, D. Barnes, M. O'Hara, Treatment of a RDX-TNT waste from a munition factory, in: *Proceeding of the 39th Industrial Waste Conference*, 1984, pp. 837–842.
- [9] D.J. Freeman, Continuous fixation and removal of explosive wastes from pink water using surfactant technology, in: *Proceeding of the 40th Industrial Waste Conference*, 1985, pp. 659–675.
- [10] J.C. Hoffsommer, J.M. Rosen, Hydrolysis of explosives in sea water, *Bull. Environ. Contam. Toxicol.* 10 (1973) 78–79.
- [11] J.L. Osmon, R.F. Klausmeier, The microbial degradation of explosives, *Dev. Ind. Microbiol.* 14 (1972) 247–252.
- [12] N.G. McCormick, J.H. Cornell, A.M. Kaplan, Biodegradation of hexahydro-1,3,5-trinitro-1,3,5-triazine, *Appl. Environ. Microbiol.* 42 (1981) 817–823.
- [13] T. Urbanski, *Chemistry and Technology of Explosives*, Programon Press, Oxford, 1977, pp. 13–77.
- [14] J. Hawari, A. Halasz, T. Sheremata, S. Beaudet, C. Groom, L. Paquet, C. Rhofir, G. Ampleman, S. Thiboutot, Characterization of metabolites during biodegradation of hexahydro-1,3,5-trinitro-1,3,5-triazine (RDX) with municipal anaerobic sludge, *Appl. Environ. Microbiol.* 66 (2000) 2652–2657.
- [15] T.L. Johnson, M.M. Scherer, P.G. Tratnyek, Kinetics of halogenated organic compound degradation by iron metal, *Environ. Sci. Technol.* 30 (1996) 2634–2640.
- [16] S.F. Cheng, S.C. Wu, The enhancement methods for the degradation of TCE by zero-valent metals, *Chemosphere* 41 (2000) 1263–1270.
- [17] G. Antoine, Degradation of benomyl, picloram, and dicamba in a conical apparatus by zero-valent iron power, *Chemosphere* 43 (2001) 1109–1117.
- [18] A. Ghauch, Degradation of benomyl, picloram, and dicamba in a conical apparatus by zero-valent iron power, 2001.
- [19] R.W. Gillham, S.F. O'Hannesin, Enhanced degradation of halogenated aliphatics by zero-valent iron, *Ground Water* 32 (1994) 958–967.
- [20] W.S. Orth, R.W. Gillham, Dechlorination of trichloroethene in aqueous solution using  $\text{Fe}^0$ , *Environ. Sci. Technol.* 30 (1996) 66–71.
- [21] A.L. Roberts, L.A. Totten, W.A. Arnold, D.R. Burris, T.J. Campbell, Reductive elimination of chlorinated ethylenes by zero-valent metals, *Environ. Sci. Technol.* 30 (1996) 2654–2659.
- [22] P.G. Tratnyek, T.L. Johnson, M.M. Scherer, G.R. Eykholt, Remediating ground water with zero-valent metals: Chemical considerations in barrier design, *Ground Water Monitor. Remed.* 17 (1997) 108–114.
- [23] A. Agrawal, P.G. Tratnyek, Reductions of nitroaromatic compounds by zero-valent iron metal, *Environ. Sci. Technol.* 30 (1996) 153–160.
- [24] J.F. Devlin, J. Klausen, R.P. Schwarzenbach, Kinetics of nitroaromatic reduction on granular iron in recirculating bath experiments, *Environ. Sci. Technol.* 32 (1998) 1941–1947.
- [25] J. Singh, S.D. Comfort, P.J. Shea, Remediating RDX contaminated water and soil using zero-valent iron, *J. Environ. Qual.* 27 (1998) 1240–1247.
- [26] C.P. Huang, H.W. Wang, P.C. Chiu, Nitrate reduction by metallic iron, *Water Res.* 32 (1998) 2257–2264.
- [27] S.S. Talmage, D.M. Opresko, C.J. Maxwell, C.J.E. Welsh, F.M. Cretella, P.H. Reno, F.B. Daniel, Nitroaromatic munition compounds: Environmental effects and screening values, *Rev. Environ. Contam. Toxicol.* 16 (1999) 1–156.
- [28] R. Venkatapathy, D.G. Bessingpas, S. Canonica, J.A. Perlinger, Kinetics models for trichloroethylene transformation by zero-valent iron, *Appl. Catal. B. Environ.* 37 (2002) 139–159.